Atmósfera (1989), **2**, p.p. 167-180

Some statistical characteristics of El Niño/southern oscillation and North Atlantic oscillation indices

UDO SCHNEIDER * and CHRISTIAN-D. SCHÖNWIESE

J. W. Goethe University, Institute of Meteorology and Geophysics, FRG

(Manuscript received Dec. 7, 1988, in final form Feb. 24, 1989)

RESUMEN

Las variaciones interanuales del fenómeno El Niño/Oscilación del Sur (ENSO) y la Oscilación del Atlántico Norte (NAO) se analizan estadísticamente en los dominios del tiempo y frecuencia, utilizando series de tiempo de los siguientes índices mensuales: dos índices de temperatura de la superficie del Océano Pacífico que reflejan eventos de El Niño (1870-1983) y dos índices de presión al nivel del mar que indican la Oscilación del Sur (1882-1987) y la NAO (1881-1984). El análisis del espectro de varianza de estas series de tiempo (con una alta resolución espectral) en un modo "integrado" (convencional) y en otro dinámico (movible en el tiempo) está basado en los dos métodos, de auto-covarianza y en el de máxima entropía. El espectro de varianza "integrado" revela picos significativos para periodos de 2.3, 2.9, 3.5 y 6 años para los índices del ENSO y de 1.7, 2.2 y 7.5 para el índice de la NAO. Algunas de estas características expectrales aparecen como casi-estacionarias desde el punto de vista dinámico, los resultados estadísticos son útiles en la identificación e interpretación de mecanismos físicos asociados con estos patrones de circulación atmosférica y oceánica de gran escala, particularmente con respecto al papel importante que la dinámica de ondas oceánicas juega en el ciclo del ENSO.

ABSTRACT

The interannual variations of the El Niño/Southern Oscillation phenomenon (ENSO) and the North Atlantic Oscillation (NAO) are statistically analysed in the time and frequency domain using time series of the following monthly indices: Two Pacific sea surface temperature indices reflecting the El Niño events (1870-1983) and two sea level pressure indices monitoring the Southern Oscillation (1882-1987) and the NAO (1881-1984). The variance spectrum analysis of these time series (with a high spectral resolution) in an "integrated" (conventional) and a "dynamic" (moving with time) way is based on both the autocovariance and the maximum entropy method. The "integrated" variance spectra reveal significant peaks at periods of 2.3, 2.9, 3.5 and 6 years for the ENSO indices and of 1.7, 2.2 and 7.5 years for the NAO index. Some of these spectral features appear to be quasi-stationary in the "dynamic" view. The statistical results are helpful in identifying and interpreting physical mechanisms associated with these large-scale oceanic/ atmospheric circulation patterns, particularly with respect to the important role of oceanic wave dynamics in the ENSO cycle.

1. Introduction

The interannual variations of the El Niño/Southern Oscillation phenomenon (ENSO) and the North Atlantic Oscillation (NAO) which represent two modes of internal climate variability are considered.

ENSO, a coupled oceanic/atmospheric phenomenon, is one of the most prominent signals of the short-term internal climate variability. Its atmospheric component, the Southern Oscillation (SO), is primarily manifest in the out-of-phase relationship between sea level pressure (SLP) variations in the south-eastern Pacific and the Indonesian region and is associated with large-scale changes in the tropical atmospheric circulation. Variations in the state of the SO are generally monitored by indices based on SLP at selected stations (Wright, 1975; Trenberth, 1976; Chen, 1982). Its oceanic part is characterized by large-scale interannual changes of the sea surface temperature (SST) in the

* Now German Weather Service, Central Office, FRG.

tropical Pacific. The SST variations are most pronounced in the eastern equatorial Pacific, revealing substantial warm events, which are known as El Niño, and cold episodes. These contrasting episodes are considered as phases of a self-sustaining cycle, the ENSO cycle, in some recent studies (Cane and Zebiak, 1985; Zebiak and Cane, 1987; Graham and White, 1988). The El Niño events are accompanied by climatic anomalies on a near-global scale (Horel and Wallace, 1981; Rasmusson and Wallace, 1983; Philander and Rasmusson, 1985). The NAO is defined as the out-of-phase relationship between SLP fluctuations in the Azores high and the Icelandic low and is associated with variations of the atmospheric flow in the intermediate area (Glowienka-Hense, 1985). It is suggested that the NAO influences the climatic conditions over western Europe and the eastern United States (Moses *et al.*, 1987). There are a number of ENSO and NAO studies using model simulations or statistical time domain assessments, but only a few address the frequency domain statistics. The previous spectral investigations (e.g., Trenberth, 1976; Julian and Chervin, 1978; Chen, 1982) are generally based on relatively short time series and allow, in consequence, only a low spectral resolution. In contrast to these previous papers, the present study is based on long time series of indices for El Niño (alternatively SST1 and SST2), the Southern Oscillation (SOI) and the North Atlantic Oscillation (NAOI), allowing a more detailed analysis of their statistical characteristics in the time and frequency domain (recurrence intervals and periodicities, respectively). In addition to an "integrated" variance spectrum analysis by means of two different techniques, autocovariance spectral analysis (ASA) and maximum entropy spectral analysis (MESA), a "dynamic" spectral analysis is performed. Some implications of the statistical results with the physical background are also discussed.

2. Data

The statistical characteristics of ENSO and the NAO are investigated using the following index time series (on a monthly basis).

a. SST1: SST anomalies in the equatorial Pacific (180°-90°W, 6°N-10°S), Jan. 1870-Dec. 1983, according to Wright (1984).

b. SST2: SST anomalies in the equatorial eastern Pacific (130°W-80°W, 0°-5°S), Jan. 1870-Dec. 1983, from Schneider and Fleer (1988).

c. SOI: SLP difference anomalies between Tahiti (17.5°S, 149.6°W) and Darwin, Australia (12.4°S, 130.9°E), normalized by the overall standard deviation (SD), Jan. 1882-Aug. 1987.

d. NAOI: SLP difference anomalies between the centers of the Azores high and Icelandic low, normalized by the overall SD, Jan. 1881-Dec. 1984.

The corrected Tahiti SLP data Jan. 1882-Dec. 1935 are from Ropelewski and Jones (1987). An additional correction of +1.0 hPa is applied to the Jan. to Dec. 1905 SLP data. The SLP data for Tahiti since Jan. 1936 and for Darwin since Jan. 1882 are obtained from the World Weather Records (WWR) and the Monthly Climatic Data For the World. Some gaps of the Tahiti SLP time series are interpolated by means of a linear regression (Jan. 1890-Dec. 1940) using the SLP data of Apia, Samoa (13.8°S, 171.8°W) (data source: WWR). The Tahiti and Apia SLP data (Jan. 1890-Dec. 1940) reveal a correlation coefficient of 0.39, which exceeds (taking the autocorrelation into account) the 99% confidence level.

Monthly SLP data representing the core regions of the Azores high and Icelandic low Jan. 1881-Dec. 1984 are provided by Glowienka-Hense (1987).

The indices are calculated as deviations from a 30-year lowpass filtered annual cycle. This method is very effective in removing the (even slowly varying) annual cycle and filtering out long-term variations (with periods longer than 30 years). It is comparable to the procedure described by Luther and Harrison (1984) except that the anomalies represent departures from a low-pass filtered and not from a running-mean annual cycle.

3. Time Domain Analysis

3.1 A Conceptional Framework of the ENSO Cycle

Many ENSO studies are performed using model simulations or observational statistics. Most of the earlier investigations, however, are focused on the warm events that represent only a part of the full ENSO cycle. In more recent analyses the warm and cold episodes are considered as phases of a self-sustaining ENSO cycle. In the mean state the tropical Pacific is warm in the west and cold in the east. In association with this SST distribution there is an atmospheric convergence over the pool of warm water in the west Pacific/Indonesian region and a divergence in the region of the southeastern Pacific. The easterly Pacific trade winds blowing towards the convergence zone drive warm surface water westward that is accumulated in the western Pacific and cause the upwelling of cold sub-surface water in the east, thus maintaining the zonal temperature contrast responsible for the atmospheric circulation. In response to that, the thermocline that separates the warm mixed layer of the ocean from the deeper cold stratified water is deep (~150 m) in the western part but near the surface in the eastern part of the Pacific. The feedback between the SST, surface wind and atmospheric convergence patterns is in general positive, although it is varying through the year (Philander *et al.*, 1984; Wright, 1985). These seasonal variations of the feedback which is strong during (northern) summer and autumn and weak during winter and spring can account for the phase-locking of the warm events to the annual cycle and modulate the development of the warm events (see e.g., Wright, 1985; Zebiak and Cane, 1987). The development of the warm and cold episodes is briefly described in terms of deviations from the mean state. (For a comprehensive description of the warm events see the composit- studies of Rasmusson and Carpenter (1982) and Schneider and Fleer (1988)). In addition to that, some aspects of the coupled ENSO cycle shall be discussed.

The warm events generally set in during the (northern) spring and are marked by substantial positive SST anomalies at the South American west coast. These warm anomalies are induced by eastward propagating oceanic equatorial (downwelling) Kelvin waves, which are forced by westerly wind anomalies as hypothesized by Wyrtki (1975). This hypothesis is supported by model simulations (McCreary, 1976; Philander, 1981) and by very recent sea level studies based on satellite imagery (Miller *et al.*, 1987; Cheney and Miller, 1988).

Several investigations point to the importance of westerly wind anomalies (or westerly wind bursts) in the western Pacific for the initiation of the warm events (Luther *et al.*, 1983; Luther and Harrison, 1984; Gutzler and Harrison, 1987). Interactions between SST and surface wind anomalies in the region of the South Pacific Convergence Zone (SPCZ) appear to play an important role in this context (e.g., Trenberth and Shea, 1987; Schneider and Fleer, 1988; Von Storch *et al.*, 1988). The (first baroclinic mode) equatorial downwelling Kelvin waves cross the Pacific in 2 to 3 months,

depress the thermocline in the eastern Pacific and cause an anomalous eastward transport of heat, thus resulting in the initial positive SST anomalies in the equatorial eastern Pacific (Cane, 1983; Gill, 1983; Harrison and Schopf, 1984). The warm anomaly intensifies and is spreading westward along the equator to the dateline due to interactions between the SST, surface wind and convergence patterns. The warm anomaly which is accompanied by westerly wind anomalies (weakened trade winds) reaches its maximum extent during winter, covering nearly the entire equatorial Pacific Ocean.

A cold anomaly which appears at the South American west coast during the next spring indicates the transition from the warm to the cold phase. This negative SST anomaly again increases and is expanding westward along the equator. The cold episode which is characterized by easterly wind anomalies (strengthened trade winds) is maintained until the initiation of the next warm event.

Although the development of either the warm and cold episodes can be satisfactorily described by interactions between SST, surface wind and convergence patterns, these positive feedback processes cannot explain the transitions from one state to the other. In order to account for the oscillatory behaviour of the coupled Pacific Ocean/atmosphere system a negative feedback mechanism that controls the positive feedback processes described above is necessary.

Recent studies (Wyrtki, 1985; Cane and Zebiak, 1985; Zebiak and Cane, 1987) indicate that variations in the heat content of the oceanic mixed layer may play the role of a lagged negative feedback mechanism. There is a buildup in equatorial heat content, especially in the western Pacific, prior to the onset and a rapid decrease during the course of the warm event. The warm events are not only characterized by a redistribution of heat from the western to the eastern Pacific, but the warm upper layer of the equatorial Pacific also looses heat by enhanced evaporation (to the atmosphere) and by an anomalous oceanic poleward heat transport (by northward and southward propagating coastal Kelvin waves that are generated by the reflection of the equatorial Kelvin waves at the South American west coast). During the cold episodes the oceanic upper layer heat reservoir, particularly in the western Pacific, is slowly refilled. Until this heat reservoir is sufficiently refilled, there is not enough warm water to sustain a warm event.

Graham and White (1988) recognized the important influence of oceanic off-equatorial Rossby waves on the upper layer heat content. The possible role of the off-equatorial Rossby waves in the ENSO cycle is discussed in the concluding section.

3.2 ENSO Indices

The time series of the 12-month Gaussian low-pass filtered SOI and SST indices are presented in Figure 1. They show coherent fluctuations reflecting quite well the interannual SST and SLP variations associated with ENSO. The El Niño events coincide with phases of low SOI values and are generally preceded by periods of high SOI values as is obvious from Figure 1. Periods of high (low) SOI values reflect an increased (decreased) zonal SLP gradient between the southeastern Pacific and the Indonesian region and are associated with strengthened (weakened) Pacific trade winds and negative (positive) SST anomalies. The subsequent drop (rise) of the SOI indicates a relaxation (intensification) of the zonal SLP gradient which is accompanied by a weakening (strengthening) of the trade winds and marks the transition from the cold (warm) phase into the other.

The years of El Niño events are available from Figure 1 or more precisely, from the warm event catalogues published by Van Loon and Shea (1985), Quinn *et al.* (1987) and Schneider and Fleer (1988). The most recent ENSO event 1986/87 is indicated by the negative SOI values. The warm

events occur at intervals from 2 to 8 years with a prefered recurrence interval of 3 to 4 years. The 1877/78 and 1982/83 episodes represent the strongest warm events recorded (see also Kiladis and Diaz, 1986). During the 1982/83 event the SOI dropped to its lowest value (-3.9 in Feb. 1983).

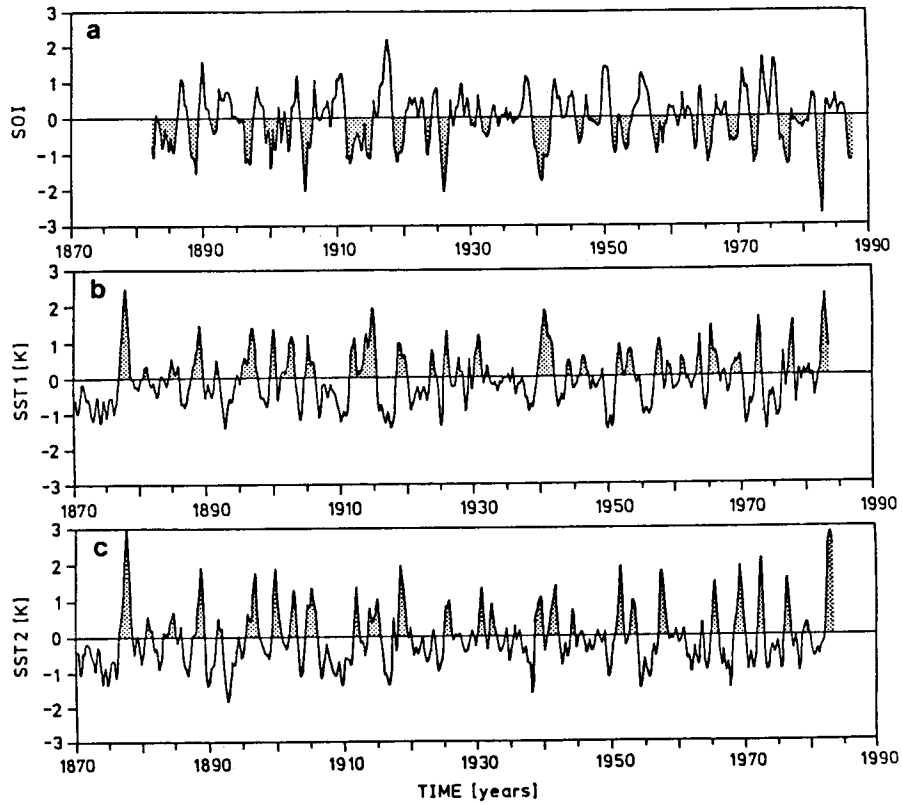

Fig. 1. 12-month Gaussian low-pass filtered time series of a) SOI (SD), b) SST1 index (K) and c) SST2 index (K).

3.3. NAO Index

The time series of the 12-month Gaussian low-pass filtered NAOI, which is presented in Figure 2, exhibits a relatively large short-term variability but also long-term fluctuations. Periods of extreme (high or low) NAOI occur at very irregular intervals. Years of high ($\geq$1.0) NAOI values are 1881, 1890, 1894, 1903, 1913, 1938, 1957 and 1976, whereas 1888, 1917, 1956 and 1969 represent years of low

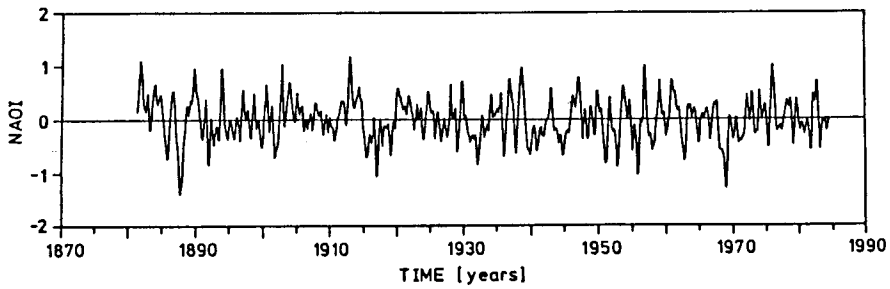

Fig. 2. 12-month Gaussian low-pass filtered time series of the NAO index (SD).

($\leq$ 1.0) NAOI values. A high (low) NAOI is associated with a strengthened (weakened) meridional SLP gradient between the Azores high and Icelandic low and intensified (weakened) westerly flow over the northern Atlantic.

4. Frequency Domain Analysis

4.1 General Remarks

The "integrated" variance spectra of the time series are computed using two different techniques: the ASA method, based on the Fourier transform of the autocovariance function (Blackman and Tukey, 1958), and the MESA method (Burg, 1967, 1972). In order to obtain comparable relative spectral estimates, the variance spectral estimates are divided by the total variance. (Note, however, that the average relative variance in each spectral estimate is lower for the MESA method than for the ASA method due to its higher spectral resolution). The statistical confidence of the sample spectral peaks is tested using a first order autoregressive Markov process (red noise) and χ^2-tests (Mitchell *et al.*, 1966) for the ASA method and, following Livezey and Chen (1983), Monte Carlo tests based on random time series (with the persistence of the observed time series) for the MESA method. In addition to the "integrated" variance spectra, a "dynamic" (moving with time) variance spectrum analysis is applied to the time series of the indices in order to study the temporal behaviour of the variance spectra (method and discussion see Schönwiese, 1987).

The cross spectrum components, the cospectrum and quadrature-spectrum, which are obtained by a Fourier transform of the even and odd parts of the cross covariance function, as well as the amplitude, phase and squared coherence spectra are calculated as described by Jenkins and Watts (1968). Additionally, the confidence levels of the squared coherence are estimated according to Julian (1975).

The graphs of all variance spectra and cross spectrum components of the index time series are truncated at periods shorter than 12 months because only interannual variations are considered here.

4.2 ENSO Indices

The "integrated" variance spectra (ASA: maximum lag=360; MESA: 180 coefficients, 540 frequencies) of the unfiltered time series of the monthly SOI (1272 values, 6.6 degrees of freedom (DF)) and SST indices (1368 values, 7.1 DF) which are shown in Figure 3 are quite similar for the ASA and the MESA method. The spectra contain the dominant variance in the period range of approximately 27 to 96 months (2.2 to 8 years), which corresponds to the typical period range of ENSO (Trenberth, 1976; Julian and Chervin, 1978; Chen, 1982). The variance spectra of all three ENSO indices exhibit essentially the same peaks (significant at the 95% or 99% confidence levels) centered at periods of 28, 34, 42 and 72 months (2.3, 2.9, 3.5 and 6 years). The peak at 28 months, which reflects the quasi-biennial oscillation (QBO), is less pronounced in the spectra of the SST indices than in the spectrum of the SOI series.

The "dynamic" variance spectra (ASA: maximum lag=180) of the subinterval time series of the monthly ENSO indices (600 values, 6.2 DF) which are plotted in terms of the confidence levels exceeded are shown in Figure 4. They reveal that the variance maxima at 28, 42 (not for SST1) and, most pronounced, at 72 months, although they show slight variations in the period and/or bandwidth, are relatively stable over the whole time interval. These spectral peaks, especially at 72

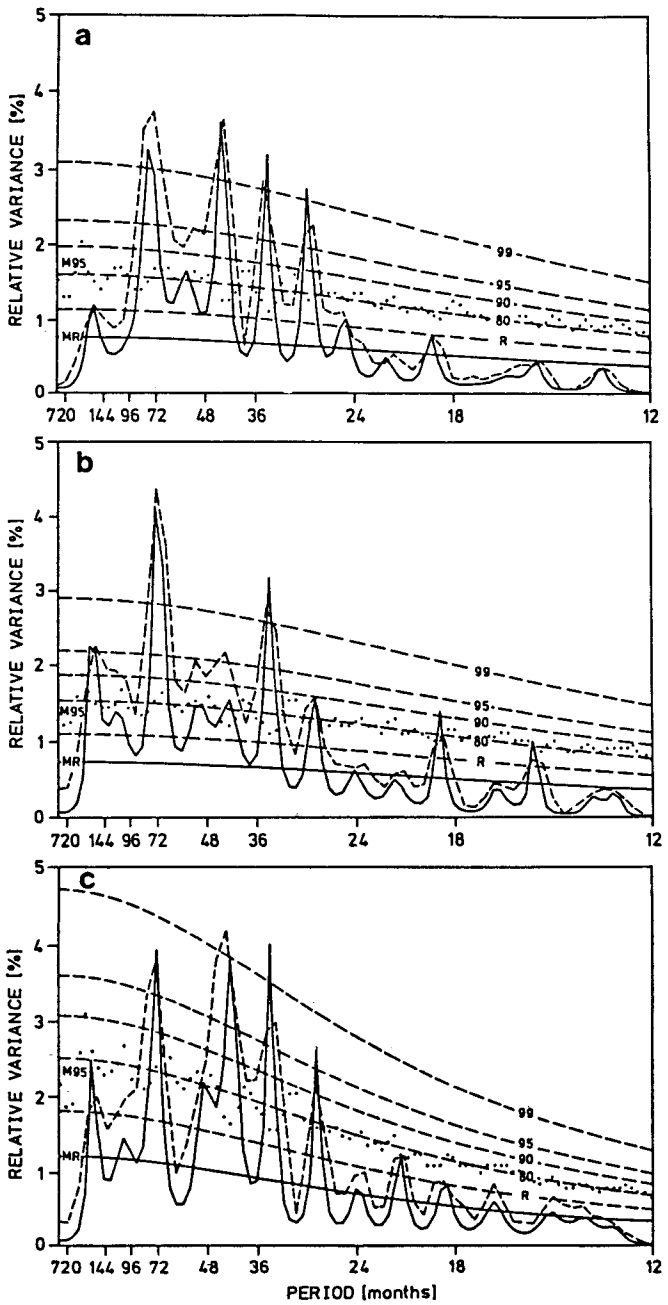

Fig. 3. Variance spectra (ASA dashed, MESA solid) of the time series of monthly a) SOI, b) SST1 index and c) SST2 index. The ASA red noise and 80% to 99% confidence levels (dashed) based on χ^2-tests are denoted by R and 80, .., 99. MR (solid) and M95 (dotted) specify the MESA red noise and 95% confidence level based on 1000 random time series. (ASA = autocorrelations, MESA = Maximum entropy spectral analysis).

months, are significant (at the 95% or 99% confidence levels) over most time subintervals, whereas the peak at 34 months occurs only during a few subintervals. It is important to note, however, that only the first and last subinterval time series are absolutely independent from each other.

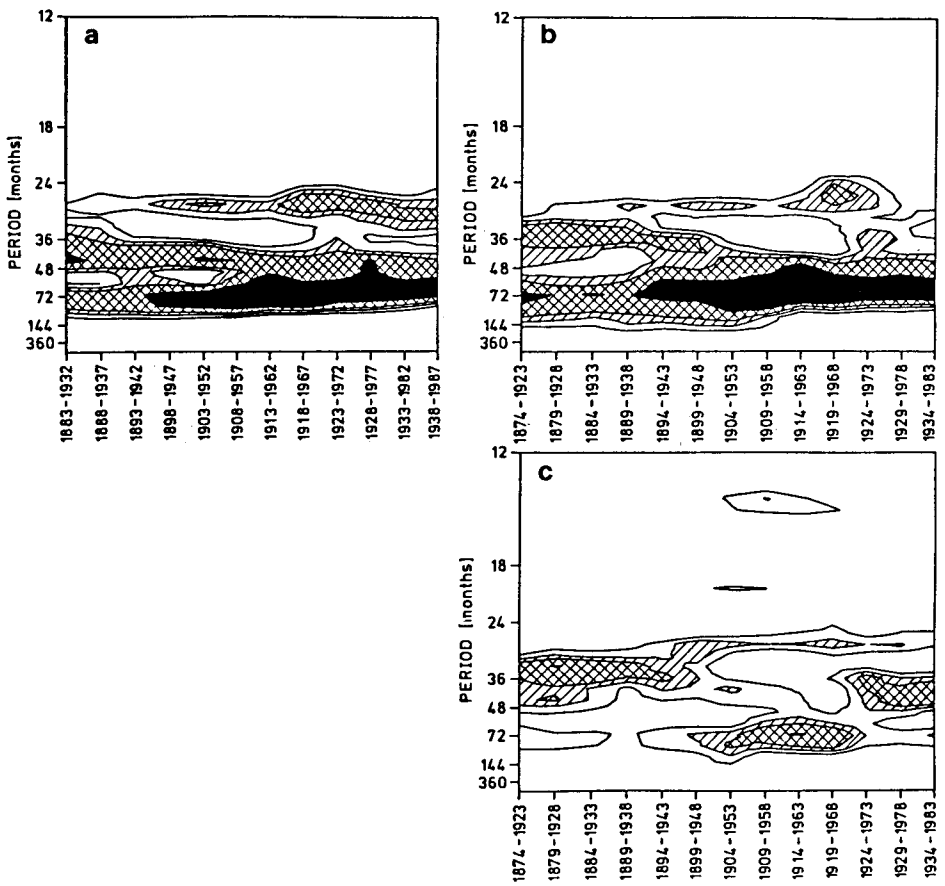

Fig. 4. Dynamic variance spectra (ASA) of the time series of monthly a) SOI, b) SST1 index and c) SST2 index. The contour lines indicate the confidence levels exceeded (≥ 99% black, ≥ 95% cross-hatched, ≥ 90% hatched, ≥ 80% white).

A cross spectrum analysis, which is performed in order to study the relationship between the ENSO indices in the frequency domain, confirms some aspects of the previously described ENSO cycle. The squared coherence, amplitude and phase spectra (maximum lag=180) between the time series of the SOI and both SST indices (1224 values, 13.1 DF) are illustrated in Figure 5. The squared coherence and amplitude spectra confirm the strong coupling between the SOI (reflecting also the large-scale variations in the Pacific trade wind field) and the SST anomalies in the ENSO period range. Over this period range the squared coherence of the SOI time series with the series of the larger-scale SST1 index is higher (significant at the 99.9% confidence level) than with the series of the SST2 index which is significant at the 99% confidence level (with a maximum at 72 months exceeding the 99.9% confidence level).

The cospectra (not shown) between the series of the SOI and SST indices are negative over this period range confirming the temporal out-of-phase relationship between them.

The phase spectra indicate that variations of the SOI coincide with opposite changes of the SST1 index, whereas they lag opposite changes of SST2 in the ENSO period range. At 72 months, for example, the SST2 index leads in respect of the SOI (SST1 index) by 5.8+2.0 (5.2+2.4) months based on a 95% confidence estimation of the phase difference (Jenkins and Watts, 1968). These phase relations reflect the observed tendency for the SST anomalies to spread westward during

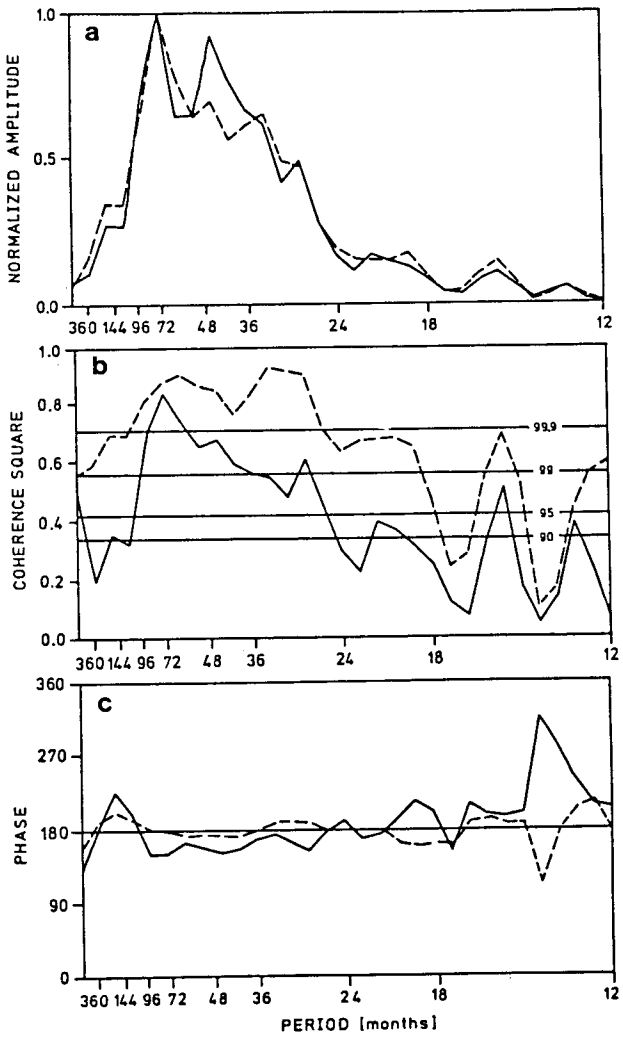

Fig. 5. a) Amplitude, b) squared coherence and c) phase spectra between the time series of monthly SOI and SST1 index (dashed) or SOI and SST2 index (solid). The 90% to 99.9% confidence levels of the squared coherence are indicated.

the warm (and cold) episodes and for the massive large-scale weakening of the Pacific trade winds (represented by the SOI) to occur simultaneously with the maximum SST anomalies in the central Pacific several months after the first appearence of the warm anomaly at the South American west coast (Rasmusson and Carpenter, 1982; Schneider and Fleer, 1988).

4.3 NOA Index

The "integrated" variance spectra (ASA: maximum lag=360; MESA: 180 coefficients, 540 frequencies) of the unsmoothed time series of the monthly NAOI (1248 monthly values, 6.4 DF) which are again very similar for the ASA and the MESA method show significant peaks (at the 95% confidence level) at periods of 21 and 26 months (1.7 and 2.2 years) (see Fig. 6).

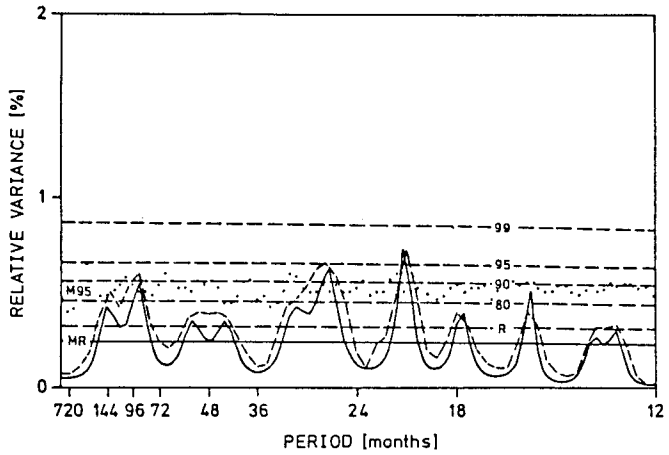

Fig. 6. As in Figure 3, but for the time series of monthly NAO index.

The "dynamic" variance spectrum (ASA: maximum lag=180) of the subinterval time series of the monthly NAOI (600 values, 6.2 DF) is shown in Figure 7. The peak at 21 months (although significant only at the 80% or 90% confidence levels) is very stable over the whole period observed, whereas the peak at about 26 months is significant (at the 95% confidence level) only during the last time subintervals. Additionally, a peak at about 90 months, which is significant at the 95% confidence level, appears during the first subintervals.

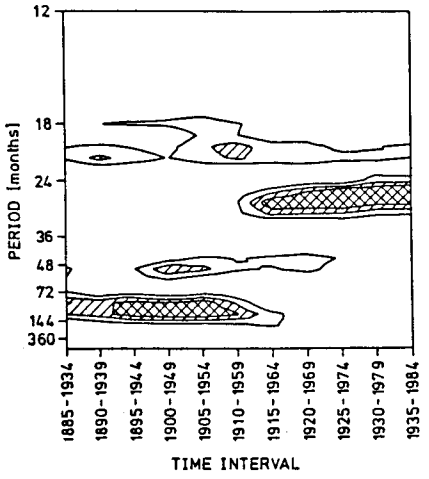

Fig. 7 As in Figure 4, but for the time series of monthly NAO index.

5. Discussion and Conclusions

Some implications of the statistical results with the physical background of ENSO and the NAO are discussed in the following.

The statistical characteristics of the ENSO indices described in chapters 3.2 and 4.2, in particular, the existence of significant peaks in the variance spectra (at 2.3, 2.9, 3.5 and 6 year periodicities) and their relative stability in time, point to the dominant role of deterministic processes in the self-

sustaining ENSO cycle. They are interpreted in the conceptual framework outlined in section 3.1, the positive feedback between SST, surface wind and convergence patterns and the role of the heat content of the upper layer of the equatorial Pacific as a delayed negative feedback mechanism.

The shortest time interval between successive warm events (2 years) is determined by the duration of a warm event (about 1 year) plus the minimum time required to sufficiently refill the heat reservoir of the warm mixed layer of the equatorial, particularly western, Pacific to sustain the next warm event (about 1 year). Although this concept agrees with the irregular recurrence of El Niño events at time intervals of 2 or more years, it cannot explain the observed quasi-periodicity.

Graham and White (1988) suggest that westward propagating off- equatorial Rossby waves provide a quasi-periodic forcing mechanism that may induce the observed quasi-periodicity. The time required by the baroclinic Rossby waves to cross the Pacific, which is 9 months near the equator, increases rapidly with latitude and reaches about 4 years at 12° latitude. The upwelling (downwelling) Rossby waves which are generated in the central Pacific away from the equator during the warm (cold) episodes (for a detailed description see Graham and White, 1988) are subsequently reflected at the western boundary of the Pacific basin into the equatorial waveguide. The reflected upwelling (downwelling) Kelvin waves may influence the heat content of the upper layer of the equatorial Pacific in a way that causes the delayed transition from the warm (cold) phase into the other.

Here it is speculated that the reflection of the off-equatorial Rossby waves into the equatorial waveguide may induce SST anomalies in the western Pacific. In accordance to the "classical" concept of the initiation of the warm events, these SST anomalies may result in wind anomalies in the western Pacific due to interactions between SST, surface wind and convergence patterns in the region of the SPCZ, which may be important for the initiation of warm events. Furthermore, it is supposed that the observed quasi-periodicity of the ENSO cycle can be satisfactorily explained by a combination of the positive feedback processes between SST, surface wind and convergence patterns and the delayed negative feedback with variations in the heat content of the upper layer of the equatorial Pacific, in which oceanic wave dynamics play a crucial role.

Periods of high or low NAOI values occur at very irregular intervals, although the variance spectra reveal significant peaks at 1.7, 2.2 and about 7.5 years, which are, in part, relatively stable in time (see sections 3.3 and 4.3).

Although the processes responsible for the NAO are largely unknown, some studies (e.g. Glowienka-Hense, 1985) suggest an influence on the NAO by the SST in the northern Atlantic. Kelly *et al.* (1986) report that variations in the Islandic low are related to changes in ice cover in the Islandic region. Angell and Korshover (1984) also find an influence of the ENSO phenomenon on the SLP and the position of the Icelandic low and Azores high.

The recent progress in describing, understanding and modelling these phenomena, especially ENSO (note the relatively successful prediction of the 1986/87 ENSO event with a coupled ocean/ atmosphere model by Cane *et al.*, 1986), provide a basis for future improvements, including long-range weather forecasting. Further investigations, however, are necessary in order to understand and model the physical processes indicated by the statistical characteristics (e.g. the specific periodicities) in more detail.

Acknowledgements

This study was supported by the German Government Climate Research Program (BMFT, Project

number KF 2012 8). The authors thank R. Glowienka-Hense for providing the NAO data and C. Ogrowsky for drawing the figures.

REFERENCES

Angell, J. K. and J. Korshover, 1984. Some long-term relations between equatorial sea-surface temperature, the four centers of action and 700 mb flow. *J. Clim. Appl. Meteor.*, **23**, 1326- 1332.

Blackman, R. B. and J. W. Tukey, 1958. The measurement of power spectra. Dover, New York.

Burg, J. P., 1967. Maximum entropy spectral analysis. Paper presented at the 37th meeting, Soc. Explor. Geophys., Oklahoma city.

Burg, J. P., 1972. The relationship between maximum entropy and maximum likelihood spectra. *Geophysics*, **37**, 375-376.

Cane, M. A., 1983. Oceanographic events during El Niño. *Science*, **222**, 1189-1195.

Cane, M. A. and S. E. Zebiak, 1985. A theory for El Niño and the Southern Oscillation. *Science*, **228**, 1085-1087.

Cane, M. A., S. E. Zebiak and S. C. Dolan, 1986. Experimental forecasts of El Niño. *Nature*, **321**, 827-832.

Chen, W. Y., 1982. Assessment of Southern Oscillation sea level pressure indices. *Mon. Wea. Rev.*, **110**, 800-807.

Cheney, R. E. and L. Miller, 1988. Mapping the 1986-87 El Niño with GEOSAT altimeter data. EOS Trans. AGU, **69**, 754-755.

Gill, A. E., 1983. An estimation of sea-level and surface current anomalies during the 1972 El Niño and consequent thermal effects. *J. Phys. Oceanogr.*, **13**, 586-606.

Glowienka-Hense, R., 1985. Studies on the variability of Icelandic low and Azores high between 1881 and 1983. *Beitr. Phys. Atmosph.*, **58**, 160-170; 1987: priv. comm.

Graham, N. E. and W. B. White, 1988. The El Niño cycle: A natural oscillator of the Pacific Ocean-atmosphere system. *Science*, **240**, 1293-1302.

Gutzler, D. S. and D. E. Harrison, 1987. The structure and evolution of seasonal wind anomalies over the near-equatorial eastern Indian and western Pacific Oceans. *Mon. Wea. Rev.*, **115**, 169-192.

Harrison, D. E. and P. S. Schopf, 1984. Kelvin-wave induced anomalous advection and the onset of surface warming in El Niño events. *Mon. Wea. Rev.*, **112**, 923-933.

Horel, J. D. and J. M. Wallace, 1981. Planetary-scale atmospheric phenomena associated with the Southern Oscillation. *Mon. Wea. Rev.*, **109**, 813-829.

Jenkins, G. M. and D. G. Watts, 1968. Spectral analysis and its applications. Holden-Day, San Francisco.

Julian, P. R., 1975. Comments on the determination of significance levels of the coherence statistic. *J. Atmos. Sci.*, **32**, 836-837.

Julian, P. R. and R. M. Chervin, 1978. A study of the Southern Oscillation and Walker Circulation phenomenon. *Mon. Wea. Rev.*, **106**, 1433-1451.

Kelly, P. M., C. M. Goodess and B. S. G. Cherry, 1986. The Icelandic sea-ice record. Climate Monitor, **15,** 11-17.

Kiladis, G. N. and H. F. Diaz, 1986. An analysis of the 1877/78 ENSO episode and comparison with 1982/83. *Mon. Wea. Rev.*, **114**. 1035-1047

Livezey, R. E. and W. Y. Chen, 1983. Statistical field significance and its determination by Monte Carlo techniques. *Mon. Wea. Rev.*, **111**, 46-59.

Luther, D. S. and D. E. Harrison, 1984. Observing long-period fluctuations of surface winds in the tropical Pacific: Initial results from island data. *Mon. Wea. Rev.*, **112**, 285-302.

Luther, D. S., D. E. Harrison and R. A. Knox, 1983. Zonal winds in the central equatorial Pacific and El Niño. *Science*, **222**, 327- 330.

McCreary, J., 1976. Eastern tropical ocean response to changing wind systems: With application to El Niño. *J. Phys. Oceanogr.*, **6,** 632-645.

Miller, L., R. E. Cheney and B. C. Douglas, 1987. GEOSAT altimeter observations of Kelvin waves and the 1986-87 El Niño. *Science*, **239,** 52-54.

Mitchell, J. M. *et al.,* 1966. Climatic change. WMO publication No. 195, Geneva.

Moses, T., G. N. Kiladis, H. F. Diaz and R. G. Barry, 1987. Characteristics and frequency of reversals in mean sea level pressure in the North Atlantic sector and their relationship to long-term temperature trends. *J. Climatol.*, **7,** 13-20.

Philander, S. G. H., 1981. The response of equatorial oceans to a relaxation of the trade wind. *J. Phys. Oceanogr.*, **11**, 176-189.

Philander, S. G. H. and E. M. Rasmusson, 1985. The Southern Oscillation and El Niño. *Adv. Geophysics*, **28A,** 197-215.

Philander, S. G. H., T. Yamagata and R. C. Pacanowski, 1984. Unstable air-sea interactions in the tropics. *J. Atmos. Sci.*, **41**, 604-613.

Quinn, W. H., V. T. Neal and S. E. A. de Mayolo, 1987. El Niño occurrences over the past four and a half centuries. *J. Geophys. Res.,* **92,** 14449-14461.

Rasmusson, E. M. and T. H. Carpenter, 1982. Variations in tropical sea surface temperature and surface wind fields associated with the Southern Oscillation/El Niño. *Mon. Wea. Rev.*, **110**, 354-3B4.

Rasmusson, E. M. and J. M. Wallace, 1983. Meteorological aspects of the El Niño/Southern Oscillation. *Science*, **222,** 1195-1202.

Ropelewski, C. F. and P. D. Jones, 1987. An extension of the Tahiti-Darwin Southern Oscillation index. *Mon. Wea. Rev.*, **115,** 2161-2165.

Schneider, U. and H. E. Fleer, 1988. Development of sea surface temperature, surface wind and divergence anomalies during a composit-ENSO episode. *Theor. Appl. Climatol.*, **39,** 146-159.

Schönwiese, C. D., 1987. Moving spectral variance and coherence analysis and some applications on long air temperature series. *J. Clim. Appl. Meteor.*, **26,** 1723-1730.

Trenberth, K. E., 1976. Spatial and temporal variations of the Southern Oscillation. *Quart. J. R. Met. Soc.*, **102,** 639-653.

Trenberth, K. E. and D. J. Shea, 1987. On the evolution of the Southern Oscillation. *Mon. Wea. Rev.*, **115**, 3078-3096.

Van Loon, H. and D. J. Shea, 1985. The Southern Oscillation. Part IV: The precursors south of 15°S to the extremes of the Oscillation. *Mon. Wea. Rev.*, **113**, 2063-2074.

Von Storch, H., H. van Loon and G. N. Kiladis, 1988. The Southern Oscillation. Part VIII: Model sensitivity to SST anomalies in the tropical and subtropical regions of the South Pacific Convergence Zone. *J. Climate*, **1**, 325-331.

Wright, P. B., 1975. An index of the Southern Oscillation. CRU RP4, Climatic Research Unit, University of East Anglia, Norwich.

Wright, P. B., 1984. Relationships between indices of the Southern Oscillation. *Mon. Wea. Rev.*, **112**, 1913-1919.

Wright, P. B., 1985. The Southern Oscillation: An ocean- atmosphere feedback system? *Bull. Amer. Met. Soc.*, **66**, 398-412

Wyrtki, K., 1975. El Niño-the dynamic response of the equatorial Pacific Ocean to atmospheric forcing. *J. Phys. Oceanogr.*, **5**, 572-584.

Wyrtki, K., 1985. Water displacements in the Pacific and the genesis of El Niño cycles. *J. Geophys. Res.*, **90**, 7129-7132.

Zebiak, S. E. and M. A. Cane, 1987. A model El Niño-Southern Oscillation. *Mon. Wea. Rev.*, **115**, 2262-2278.